Multi-target Location Based on Compressed Sensing Direct Position Determination with Missing Information

Xiangsong Huang
Harbin Engineering University
Jia Yuan
Harbin Engineering University
Zhigang Yang (zgyang@hrbeu.edu.cn)
Harbin Engineering University
Runjia Su
China Electronics Technology Group Corp 54th Research Institute

Research Article

Keywords: CSDPD, missing information, IOMP-DPD, multi-target, passive location

Posted Date: May 13th, 2022

DOI: https://doi.org/10.21203/rs.3.rs-1618117/v1

Multi-target Location Based on Compressed Sensing Direct Position Determination with Missing Information

Xiangsong Huang[1,2], Jia Yuan[1,2], Zhigang Yang[1,2](1*✉), Runjia Su[3]

1.College of Information and Communication Engineering , Harbin Engineering University, Harbin 150009, China
2.Key Laboratory of Advanced Marine Communication and Information Technology, Ministry of Industry and Information Technology, Harbin Engineering University, Harbin 150009, China
3.State Key Laboratory of satellite navigation system and equipment technology, China Electronics Technology Group Corp 54th Research Institute, Shijiazhuang 050050, China

[1] *Corresponding author (Email: zgyang@hrbeu.edu.cn)

Abstract

It often happens that we cannot acquire all information available to locate targets as obstacles exist between observation stations and targets or there is something wrong with some observation stations. Both cases are called the circumstance of missing information where partial information can be observed, resulting in poor positioning performance of multi-target location. Considering the sparse characteristic and random subsampling of Compressed Sensing (CS) theory, we think of a possibility of applying Compressed Sensing Direct Position Determination (CSDPD) to lessen the impact of missing information on multi-target location. Orthogonal matching pursuit (OMP) algorithm is a kind of greedy algorithm of CS, which can be utilized to lessen the impact of missing information. For better positioning accuracy, an improved OMP algorithm based on DPD (IOMP-DPD) is proposed through a new method of updating index set to lessen the possibility of incomplete location. It confirms by simulations that the improved method yields more accurate positioning results than OMP algorithm and outperforms than the existed MUSIC algorithm based on DPD (MUSIC-DPD), revealed in estimating more target locations in the same positioning conditions and smaller positioning errors when locating the same targets.

Keywords

CSDPD, missing information, IOMP-DPD, multi-target, passive location.

1 Introduction

Research on passive location has attracted great interest for many years. Traditional methods are usually 'two-step' methods [1] with required data obtained by various means and fused to estimate targets in the stage of data processing [2] when some target information may be lost, leading to poor positioning performance. As a result, Direct Position Determination (DPD) [3] was proposed, which is a single-step method [4], fusing data directly from all observation stations to locate targets [5]. So far, there has been various methods based on different information with DPD approach researched, such as multi-array data fusion [6], unitary space-time subspace data fusion [7], doppler shifts and angle of arrival [8], delay and doppler [9] and so on. It also has many derivative methods, such as the adaptive direct position determination [10], which provides an effective method to determine the emitter position directly. In case of time-varying channels, an adaptive sparsity-based DPD approach [11] is useful without the number of emitters as a prior, but shows great performance on location estimation accuracy. DPD algorithm has a problem on resolution [12] and computation resources in searching phase [13], so it is essential to combine it with an appropriate methods.

It can alleviate the negative effect of missing to some extent by MUSIC algorithm based on DPD (MUSIC-DPD), but the positioning performance turns worse when it comes to more loss of target information. And we have known that Compressed Sensing (CS) [14] theory is based on sparsity and random subsampling, which means less impact on location estimation with the lack of target information. So we here combine DPD with CS algorithm, such as Orthogonal Matching Pursuit (OMP) algorithm. So far, CS theory has been widely applied in passive location with lots of methods adapted from it, such as Bayesian [15], Orthogonal Matching Pursuit [16], Focal Undetermined System Solver [17] and so on. There has been various adaptive methods of them, such as the optimal structured Bayesian [18], hierarchical Bayesian [19]; OMP based on redundancy dictionary [16], block/group OMP [20], OMP algorithm based on randomly enhanced adaptive subspace pursuit [21]; regularized FOCUSS algorithm [22].

The core problem we consider in this paper is to locate multi-targets with better positioning performance under the practical circumstance of missing information. Two cases of missing information are included: complete missing information and incomplete missing information. The first case happens when a station with something wrong fails to observe any target information. Incomplete missing information happens when there is an obstacle between an observation station and a target, leading to limited observation information available to this station.

Since CS can be used to obtain and reconstruct signals based on the sparse characteristic of the signals, a possibility is considered of applying CS theory to reduce the impact of missing information on target location. Herein we apply OMP algorithm, a greedy algorithm based on CS theory, to solve the core problem mentioned above. The target number must be prior information for OMP algorithm. We apply OMP algorithm based on DPD (OMP-DPD) first and propose an improved OMP algorithm based on DPD

(IOMP-DPD) for better positioning accuracy.

2 Mathematical Description

In this section, we will introduce a positioning model based on DPD and its mathematical description.

2.1 Measurement Signal Model

Here we consider a positioning scene of locating N far-field targets that are situated at $\mathbf{P}_n=\left(x_{pn},y_{pn},0\right)^T\ \left(n=1,\cdots,N\right)$ on the ground and monitored by Q observation stations located at $\mathbf{S}_q=\left(x_{sq},y_{sq},z_{sq}\right)^T\ \left(q=1,\cdots,Q\right)$ with a uniform linear array consisting of $M\left(M>N\right)$ sensors on each station. $\left(\square\right)^T$ expresses the transposition of the argument. Let Δx be the baseline shared of Q arrays. K snapshots are adopted. N and information of stations are prior information.

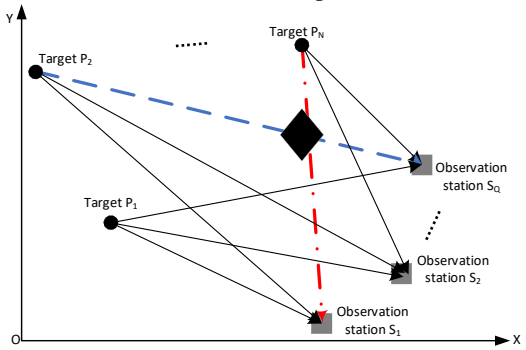

Fig. 1 Positioning scene of incomplete missing information

Fig. 1 shows a top view of the positioning scene of incomplete missing information, where the diamond, black solid dots and grey squares represent the obstacle, targets and observation stations respectively. We add the solid lines to indicate that the stations can gain information of corresponding targets just for clarity. Notice that there is an obstacle between station $\mathbf{S}_Q$ and target $\mathbf{P}_2$, which means the Q th station gains no information about the second target in this case. The observation station is called an invalid station if there is something wrong with it. The second case of missing information happens when there is an invalid station, which cannot gain any target information at all. That is, the target number N in the received signal model is actually variable for different observation stations.

Suppose N_q represents the number of targets that can be observed by the q th station. The received signal at the m th $\left(m=1,\cdots,M\right)$ sensor on the q th station can be denoted as:

$$\mathbf{x}_q\left(m\right)=\sum_{n=1}^{N_q}\mathbf{a}_{qm}\left(\mathbf{P}_n\right)\mathbf{s}\left(n\right)+\mathbf{w}_q\left(m\right) \tag{1}$$

where $\mathbf{a}_{qm}\left(\mathbf{P}_n\right)=e^{-j\frac{2\pi}{l}(m-1)\Delta x\sin\theta_{q,n}}$ is the response entry and $\theta_{q,n}$ is the azimuth between $\mathbf{P}_n$ and $\mathbf{S}_q$. $\mathbf{s}\left(n\right)$ represents the n th target signal. $\mathbf{w}_q\left(m\right)$ represents the measurement noise generated when observing targets by the m th sensor on the q th station. l is the signal wavelength. So the received signal model on the q th observation station can be stated as:

$$\mathbf{X}_q=\mathbf{A}_q\left(\mathbf{p}\right)\mathbf{s}+\mathbf{w}_q \tag{2}$$

where $\mathbf{X}_q=\left[\mathbf{x}_q\left(1\right),\cdots,\mathbf{x}_q\left(M\right)\right]^T$, $\mathbf{w}_q=\left[\mathbf{w}_q\left(1\right),\cdots,\mathbf{w}_q\left(M\right)\right]^T$ is the measurement noise vector on the q th observation station and $\mathbf{p}=\left[\mathbf{P}_1,\cdots,\mathbf{P}_{N_q}\right]^T$. $\mathbf{s}$ is the source signal. $\mathbf{A}_q\left(\mathbf{p}\right)$ is the array manifold denoted as:

$$\mathbf{A}_q\left(\mathbf{p}\right)=\left[\mathbf{a}_q\left(\mathbf{P}_1\right)\ ,\cdots,\ \mathbf{a}_q\left(\mathbf{P}_{N_q}\right)\right] \tag{3}$$

$$\begin{aligned}\mathbf{a}_q\left(\mathbf{P}_n\right)&=\left[\mathbf{a}_{q1}\left(\mathbf{P}_n\right)\ ,\ \mathbf{a}_{q2}\left(\mathbf{P}_n\right)\ ,\ \cdots\ ,\ \mathbf{a}_{qM}\left(\mathbf{P}_n\right)\right]^T\\&=\left[1,\ \exp\left(-j\frac{2\pi}{l}\Delta x\sin\theta_{q,n}\right),\ \cdots\ ,\exp\left(-j\frac{2\pi}{l}(M-1)\Delta x\sin\theta_{q,n}\right)\right]^T\end{aligned} \tag{4}$$

Then the model of the positioning scene is denoted as:

$$\mathbf{X}=\mathbf{A}\mathbf{s}+\mathbf{w} \tag{5}$$

$\mathbf{A}=\left[\mathbf{A}_1^T\left(\mathbf{p}\right)\ ,\cdots,\ \mathbf{A}_Q^T\left(\mathbf{p}\right)\right]^T$, $\mathbf{X}=\left[\mathbf{X}_1^T,\cdots,\mathbf{X}_Q^T\right]^T$, $\mathbf{w}=\left[\mathbf{w}_1^T,\cdots,\mathbf{w}_Q^T\right]^T$.

2.2 Sparse Representation

Divide the observation area into G grids with G_X equal parts in a line and G_Y in a column and each grid represents the position of a potential target $\tilde{\mathbf{P}}_g=\left(x_g,y_g,0\right)^T\ \left(g=1,\cdots,G\right)$. Here $\tilde{\square}$ indicates that the argument is related to the potential targets. Similarly, the potential source signal can be expressed by a $G\times1$ vector $\tilde{\mathbf{s}}$, where nonzero elements represent the real target locations. $\tilde{\mathbf{s}}$ is a sparse vector since $N\ll G$. What we seek to solve actually is to find the grid indexes corresponding to the nonzero elements. Suppose any two real targets are at least as far as two grids apart to prevent the observation station from identifying them as the same target. Similarly, array manifold corresponding to $\tilde{\mathbf{s}}$ is:

$$\tilde{\mathbf{A}}_q\left(\tilde{\mathbf{p}}\right)=\left[\tilde{\mathbf{a}}_q\left(\tilde{\mathbf{P}}_1\right),\cdots,\tilde{\mathbf{a}}_q\left(\tilde{\mathbf{P}}_G\right)\right] \tag{6}$$

$$\begin{aligned}\tilde{\mathbf{a}}_q\left(\tilde{\mathbf{P}}_g\right)&=\left[\tilde{\mathbf{a}}_{q1}\left(\tilde{\mathbf{P}}_g\right),\tilde{\mathbf{a}}_{q2}\left(\tilde{\mathbf{P}}_g\right),\cdots,\tilde{\mathbf{a}}_{qM}\left(\tilde{\mathbf{P}}_g\right)\right]^T\\&=\left[1,\ e^{-j\frac{2\pi}{l}\Delta x\sin\theta_{q,g}},\ \cdots\ ,e^{-j\frac{2\pi}{l}(M-1)\Delta x\sin\theta_{q,g}}\right]^T\end{aligned} \tag{7}$$

Therefore $\mathbf{X}_q$ can be expressed in another way as:

$$\mathbf{X}_q=\tilde{\mathbf{A}}_q(\tilde{\mathbf{p}})\tilde{\mathbf{s}}+\tilde{\mathbf{w}}_q \tag{8}$$

$\tilde{\mathbf{w}}_q=\left[\tilde{\mathbf{w}}_q\left(1\right),\cdots,\tilde{\mathbf{w}}_q\left(M\right)\right]^T$ is the measurement noise vector.

3 Compressed Sensing DPD (CSDPD)

What we seek to solve is to reconstruct the sparse signal.Supposing the signal and noise are uncorrelated and the noise is white noise with zero mean and variance σ_q^2. The covariance matrix of received signal $\mathbf{X}_q$ is:

$$\mathbf{R}_{\mathbf{XX}}^{(q)}=E[\mathbf{X}_q\mathbf{X}_q^H] \tag{9}$$

$\left(\square\right)^H$ denoted the conjugate transpose of the argument. In practice, the covariance matrix is obtained as:

$$\mathbf{R}_{\mathbf{XX}}^{(q)}=\frac{1}{K}\sum_{k=1}^{K}\mathbf{x}_{qk}\mathbf{x}_{qk}^H=\frac{1}{K}\mathbf{X}_q\mathbf{X}_q^H \tag{10}$$

where $\mathbf{x}_{qk}$ is the received signal on the q th observation station at the k th snapshot.

3.1 Sparse Observation Vector

Substitute (8) into (9):

$$\mathbf{R}_{\mathbf{XX}}^{(q)}=\tilde{\mathbf{A}}_q\left(\tilde{\mathbf{p}}\right)\mathbf{R}_{\mathbf{s}}\ \tilde{\mathbf{A}}_q^H\left(\tilde{\mathbf{p}}\right)\ +\ \sigma_q^2\ \mathbf{I}_M \tag{11}$$

where $\mathbf{R}_{\tilde{\mathbf{s}}} = E[\tilde{\mathbf{s}}\tilde{\mathbf{s}}^H]$ is the signal covariance matrix. $\mathbf{I}_M \in \square^{M\times M}$ is a unit matrix. Obviously, $\mathbf{R}_{\tilde{\mathbf{s}}}$ is a N -row-sparse matrix.

Let $\mathbf{B}_q = \mathbf{R}_{\tilde{\mathbf{s}}}\tilde{\mathbf{A}}_q^H(\tilde{\mathbf{p}}) \in \square^{G\times M}$ whose columns can be represented by a set of basis vectors $\{\tilde{\mathbf{a}}_q(\tilde{\mathbf{P}}_g)\}_{g=1,\cdots,G}$ approximatively. $\mathbf{B}_1,\cdots,\mathbf{B}_Q$ have the same sparsity structure obviously. Then, $\tilde{\mathbf{A}}_q(\tilde{\mathbf{p}})\mathbf{B}_q = \mathbf{R}_{\mathbf{XX}}^{(q)} - \sigma_q^2\mathbf{I}_M$ can be regarded as a matrix including the set of sparse observation vector. Hence an entry of the sparse observation vector can be denoted as:

$$\mathbf{d}_{qm} = \mathbf{r}_{qm} - \sigma_q^2\mathbf{e}_m \quad (q = 1,\cdots,Q \quad m = 1,\cdots,M) \tag{12}$$

where $\mathbf{r}_{qm}$ is the m th column of $\mathbf{R}_{\mathbf{XX}}^{(q)}$, $\mathbf{e}_m$ is the m th column of $\mathbf{I}_M$. The sparse observation vector obtained by the q th station is $\mathbf{d}_q = \left[\mathbf{d}_{q1}^H,\cdots,\mathbf{d}_{qM}^H\right]$. Therefore, the sparse observation vector can be denoted as:

$$\mathbf{d} = \left[\mathbf{d}_1,\cdots,\mathbf{d}_Q\right]^H \tag{13}$$

3.2 Dictionary Matrix

Let $\mathbf{b}$ indicate the sparse structure of $\mathbf{B}_1,\cdots,\mathbf{B}_Q$ and convert the core problem into reconstruct $\mathbf{b}$ basing on CS. The basic formula of solution is therefore denoted as:

$$\mathbf{d}_{qm} = \Psi_{qm}\mathbf{b} + \boldsymbol{\varepsilon}_{qm} \tag{14}$$

where $\boldsymbol{\varepsilon}_{qm}$ is the estimation noise vector when locating targets by the m th sensor on the q th observation station. Ψ_{qm} is an entry of the dictionary matrix designed according to $\mathbf{d}_{qm}$ and corresponds to a potential target:

$$\begin{aligned}\Psi_{qm} &= \left[\tilde{\mathbf{a}}_{q1}\mathbf{B}_q(1,m) \ ,\cdots, \ \tilde{\mathbf{a}}_{qG}\mathbf{B}_q(G,m)\right] \\ &= \left[\frac{\tilde{\mathbf{a}}_{q1}\tilde{\mathbf{a}}_{q1}^H\mathbf{d}_{qm}}{\tilde{\mathbf{a}}_{q1}^H\tilde{\mathbf{a}}_{q1}} \ ,\cdots, \ \frac{\tilde{\mathbf{a}}_{qG}\tilde{\mathbf{a}}_{qG}^H\mathbf{d}_{qm}}{\tilde{\mathbf{a}}_{qG}^H\tilde{\mathbf{a}}_{qG}}\right]\end{aligned} \tag{15}$$

where $\tilde{\mathbf{a}}_{qg}(g = 1,\cdots,G)$ is the g th column of $\tilde{\mathbf{A}}_q(\tilde{\mathbf{p}})$ and $\mathbf{B}_q(g,m)$ is the (g,m) th element of $\mathbf{B}_q$.

Likewise, $\Psi_q = \left[\Psi_{q1}^H,\cdots,\Psi_{qM}^H\right]$, $\boldsymbol{\varepsilon}_q = \left[\boldsymbol{\varepsilon}_{q1}^H,\cdots,\boldsymbol{\varepsilon}_{qM}^H\right]$. The model of target location based on CSDPD can be denoted as:

$$\mathbf{d} = \Psi\mathbf{b} + \boldsymbol{\varepsilon} \tag{16}$$

where

$$\begin{aligned}\Psi &= \left[\Psi_1,\cdots,\Psi_Q\right]^H \\ \boldsymbol{\varepsilon} &= \left[\boldsymbol{\varepsilon}_1,\cdots,\boldsymbol{\varepsilon}_Q\right]^H\end{aligned} \tag{17}$$

4 Improved OMP Algorithm Based on DPD

4.1 OMP-DPD

OMP algorithm is a kind of greedy algorithm, the principle of which is to pick an entry of the dictionary Ψ as an atom that best matches the signal residual at each iteration to avoid local optimum, update index set and atomic set, calculate signal residual based on Least Squares (LS) algorithm and iterate repeatedly until the ending condition is satisfied.

Let $\boldsymbol{\gamma}_t$ be the residual at the t th iteration and Λ_t be the index set whose entry β_t is solved by:

$$\beta_t = \arg\max_{g=1,\cdots,G}\left|\left\langle\boldsymbol{\gamma}_{t-1},\Psi_g\right\rangle\right| \tag{18}$$

Set $\Lambda_0 = \phi$, $\Phi_0 = \phi$ and $\boldsymbol{\gamma}_0 = \mathbf{d}$ as the initial condition, where ϕ denotes an empty set. Φ_t is the atomic set.

From $t = 1$, update the index set and the atomic set:

$$\Lambda_t = \Lambda_{t-1} \cup \{\beta_t\} \tag{19}$$

$$\Phi_t = \Phi_{t-1} \cup \{\Psi_{\beta_t}\} \tag{20}$$

where Ψ_{β_t} is the β_t th column of Ψ.

Calculate the sparse signal estimation based on LS:

$$\hat{\mathbf{b}}_t = \arg\min_{\mathbf{b}_t}\left\|\mathbf{d} - \Phi_t\mathbf{b}_t\right\| \tag{21}$$

$$\boldsymbol{\gamma}_t = \mathbf{d} - \Phi_t\hat{\mathbf{b}}_t \tag{22}$$

As the sparsity N is known to us, we can iterate (18), (19), (20), (21) and (22) until iterating N times.

4.2 IOMP-DPD

4.2.1 Background: Incomplete Location

Incomplete location occurs when the target number we estimate is less than that of real targets since there are several indexes of adjacent grids merged into one index while updating index set, which motivates us to seek an improved method of choosing indexes of potential targets.

4.2.2 Related Definitions

Several definitions are made as follows: the amplitude that exceeds one fifth of the maximum amplitude is called the local maximum and its corresponding grid is a local maximum grid (LMG). The grid corresponding to a real target is called a target grid (TG). We can observe that adjacent LMGs are nearly G_Y grids apart, which can be confirmed in Fig. 2. Hence, we divide G grids into G_X groups with G_Y grids on each group and the β_t that we need to update the index set is absolutely a LMG.

Actually, the calculation result of $\left|\left\langle\boldsymbol{\gamma}_{t-1},\Psi\right\rangle\right|$ does not exactly show the contribution of each column of Ψ to the sparse observation vector owning to noise and other factors. Multiple local convergence processes are carried out in practical and each converges to a TG during each iteration.

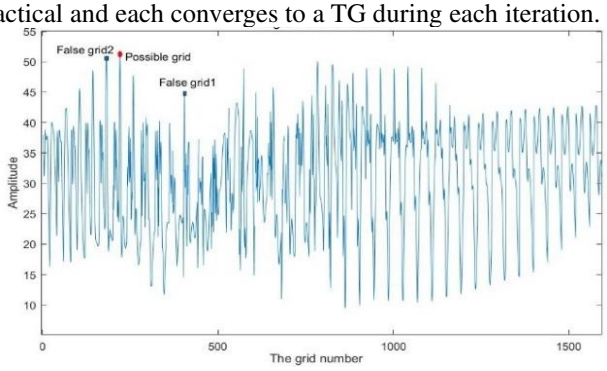

Fig. 2 A diagram of $\left|\left\langle\boldsymbol{\gamma}_{t_1-1},\Psi\right\rangle\right|$ at one iteration

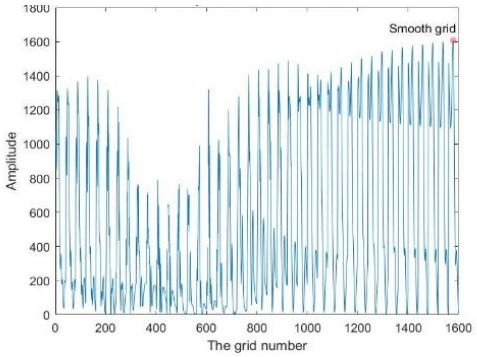

Fig. 3 Diagram of $\left|\left\langle\boldsymbol{\gamma}_{t_2-1},\Psi\right\rangle\right|$ at another iteration

Three types of LMGs are illustrated in Fig. 2 and Fig. 3, two marked diagram of $\left|\left\langle \boldsymbol{\gamma}_{t_i-1}, \Psi \right\rangle\right| \left(i = 1, 2\right)$.

There are two forms of false grid: interference false grid and second-largest-value false grid. The former is a peak grid in a local area disobeying the convergence process. Second-largest-value false grid is the grid that has the second largest amplitude and the peak amplitude after we screening the largest amplitude at the previous iterations.

Smooth grid is the peak of all amplitudes but not a convergence point in its local area, as marked in Fig. 3.

Possible grid corresponds to the amplitude which is not only the local convergence value but also the global maximum value of Λ_t which can be chosen as the β_t.

4.2.3 Improvement Method of updating index set

The core idea of IOMP is an improved method of choosing appropriate grid as β_t to update index set Λ_t by excluding false grids and smooth grids.

The index set can be written as $\Lambda_t = \left[\Lambda_{t1}, \Lambda_{t2}, \cdots, \Lambda_{tG_X}\right]$ after grouping. Pick the maximum value v_{ti} of each Λ_{ti} to form a maximum vector $\mathbf{V}_t = \left(v_{t1}, \cdots, v_{tG_X}\right)$, where

$$v_{ti} = \max\left(\Lambda_{ti}\right) \quad i = 1, \cdots, G_X \tag{23}$$

and pick the corresponding grid g_{ti} to form a grid number vector $\mathbf{g}_t = \left(g_{t1}, \cdots, g_{tG_X}\right)$. Obviously, $\Lambda_{g_{ti}} = v_{ti}$.

Let $1 \le z \le G_X$ and suppose β_t is the g_{tz} th number of $\mathbf{g}_t$, which satisfies the following conditions:

$$\begin{gathered} \Lambda_{\beta_t} = \Lambda_{g_{tz}} = \max\left(\mathbf{V}_t\right) \\ \Lambda_{g_{tz}} > \Lambda_{g_{t(z-1)}} > \Lambda_{g_{t(z-2)}} \quad , \quad \Lambda_{g_{tz}} > \Lambda_{g_{t(z+1)}} > \Lambda_{g_{t(z+2)}} \end{gathered} \tag{24}$$

Some siftings are needed to exclude the repetitive grids and second-largest-value false grids when $t \ge 2$ in case of incomplete location. Denote η as the comparison times which we need to compare β_t with all previous indexes in Λ_{t-1} and μ as the number of duplicate indexes. Obviously:

$$\eta = t - 1 \tag{25}$$

For $\ell = 1, \cdots, \eta$, we compare β_t obtained in Section A with entries of Λ_{t-1} and update $\mu = \mu + 1$ if Λ_{t-1} includes β_t. After η comparisons, the index set can be updated by adding β_t into the index set Λ_t, if and only if:

$$\mu = 0 \tag{26}$$

Otherwise, set $\Lambda_{g_{tz}} = 0$ and find β_t again if $\mu > 0$.

After that, the amplitudes corresponding to β_t and its adjacent 1 to 2 grids should be set to zero to exclude the second-largest-value false grids.

This completes the process of updating index set Λ_t at the t th iteration. Then we can update the index set $\Lambda_t = \Lambda_{t-1} \cup \left\{\beta_t\right\}$ and atomic set $\Phi_t = \Phi_{t-1} \cup \Psi_{\beta_t}$.

5 Simulations

Here we consider five targets located at $\mathbf{P}_1 = \left(35, 80, 0\right)^T km$, $\mathbf{P}_2 = \left(50, 60, 0\right)^T km$, $\mathbf{P}_3 = \left(15, 50, 0\right)^T km$, $\mathbf{P}_4 = \left(60, 10, 0\right)^T km$ and $\mathbf{P}_5 = \left(80, 40, 0\right)^T km$ among a $100km \times 100km$ square observation area with meshing step set as $2.5km$, and five observation stations located at $\mathbf{S}_1 = \left(30, 15, 30\right)^T km$, $\mathbf{S}_2 = \left(45, 25, 30\right)^T km$, $\mathbf{S}_3 = \left(35, 30, 30\right)^T km$, $\mathbf{S}_4 = \left(25, 25, 30\right)^T km$ and $\mathbf{S}_5 = \left(40, 15, 30\right)^T km$ in the air, with $M = 15$ sensors on each station. $K = 200$ snapshots are adopted and $SNR = 10dB$. Both measurement noise and estimation noise are set as white noise obeying Gaussian distribution. Positioning results based on MUSIC-DPD and IOMP-DPD algorithms are shown in figures or tables below after performing simulations 300 times.

5.1 Examples of locating multi-targets based on the above three algorithms

Fig. 4 and Fig. 5 are some examples of locating multi-targets based on OMP-DPD, IOMP-DPD and MUSCI-DPD algorithms in the same positioning conditions.

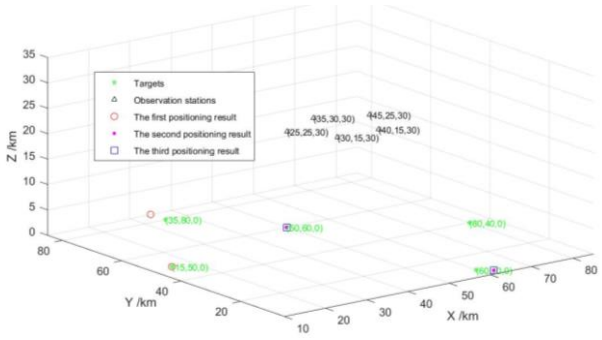

Fig. 4 Positioning results for three times based on OMP-DPD algorithm

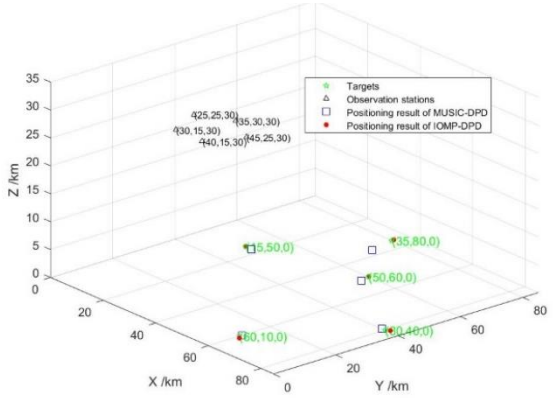

Fig. 5 Positioning results of five targets based on MUSIC-DPD and IOMP-DPD algorithms

Let green stars represent real target locations, red dots and blue squares represent positioning results of the three algorithms.

Fig. 4 shows the positioning results built on OMP-DPD for three times in the same positioning conditions, which reveals its poor positioning performance when locating multiple targets.

Fig. 5 indicates that MUSIC-DPD algorithm and IOMP-DPD algorithm are both able to locate the five targets while the former algorithm has a larger positioning deviation than the other one. Combined with two figures, the improved algorithm does have better positioning performance than OMP-DPD and MUSIC-DPD algorithms without missing information.

5.2 Complete Missing Information

In order to compare the positioning accuracy under the same conditions, we can specify which observation stations to be invalided. We disable the first observation station to

simulate the circumstance of only four effective stations, and disable the first and the second stations to simulate the circumstance of only three effective observation stations.

We denote the estimated result as $(x_{est}, y_{est}, z_{est})^T$ of the real target $(x_0, y_0, z_0)^T$, and the positioning error as:

$$Error = \sqrt{\frac{(x_{est}-x_0)^2+(y_{est}-y_0)^2+(z_{est}-z_0)^2}{x_0^2+y_0^2+z_0^2}} \times 100\% \quad (27)$$

Table 1 indicates the statistical errors of locating the five targets based on two algorithms. The error more than 10% is considered as location failure and substituted for '——'.

We can observe that all targets can be located by IOMP-DPD algorithm with only four stations accessible while it needs five observation stations when exploiting MUSIC-DPD. Also IOMP-DPD algorithm yields positioning results more closely around the real targets than the other one through the obvious comparison of positioning errors. Evidently, it is more sensitive for positioning performance of MUSIC-DPD algorithm when losing information of some observation stations. As such, IOMP-DPD performs better in case of complete missing information.

Table 1 Statistical errors with complete missing information

IOMP-DPD	The number of effective observation stations		
Error	5	4	3
Target1	0.036%	1.191%	9.824%
Target2	0.792%	3.054%	3.674%
Target3	0.000%	0.556%	1.917%
Target4	1.890%	1.091%	——
Target5	1.417%	4.456%	——
MUSIC-DPD	The number of effective observation stations		
Error	5	4	3
Target1	4.183%	7.340%	9.778%
Target2	3.306%	——	——
Target3	3.777%	4.757%	5.728%
Target4	0.781%	7.262%	——
Target5	1.397%	6.085%	5.415%

5.3 Incomplete Missing Information

Herein we consider the following four examples in Table 2, where the numbers represent the corresponding targets that can be observed by the observation stations. In the fourth example, we consider an example of combining complete missing information and incomplete missing information. Statical errors in locating the five targets in the case of incomplete missing information is shown in Table 3.

Table 2 Four examples of incomplete missing information

Targets that are not blocked	Station1	Station2	Station3	Station4	Station5
Example1	2,3,4,5	1,3,4	1,2,3,4,5	1,2,3,4,5	1,2,3,4,5
Example2	2,3,4,5	1,3,4	1,2,4,5	1,2,3,4,5	1,2,3,4,5
Example3	1,2,3	2,3,4	3,4,5	1,4,5	1,2,4,5
Example4	None	2,3,4,5	1,3,4	1,2,3,4,5	1,2,3,4,5

Table 3 Statistical errors with incomplete missing information

	Error	Example1	Example2	Example3	Example4
IOMP-DPD	Target1	0.34%	0.07%	4.45%	1.18%
	Target2	2.44%	5.87%	0.55%	3.93%
	Target3	0.00%	0.47%	——	0.03%
	Target4	5.33%	5.15%	——	1.13%
	Target5	5.94%	2.77%	——	3.14%
	Error	Example1	Example2	Example3	Example4
MUSIC-DPD	Target1	——	——	3.10%	——
	Target2	——	——	——	——
	Target3	0.60%	6.03%	——	1.32%
	Target4	2.15%	0.88%	——	1.22%
	Target5	6.97%	4.67%	——	——

From the statistical data above, we can observe that the positioning performance turns worse when there is a certain degree of missing information on each station. And it is obvious that IOMP-DPD outperforms MUSIC-DPD since it can locate more targets with all positioning errors less than 6%. Therefore, IOMP-DPD algorithm performs better than MUSIC-DPD when it comes to missing information.

5.4 Positioning Errors with Different SNR Values.

To clearly show the better performance of IOMP-DPD algorithm than that of MUSIC-DPD algorithm, we take a number every 5 from $-10dB$ to $20dB$ as the SNR values to analyze the influence of the signal-to-noise ratio on positioning performance based on the two algorithms without missing information.

Table 4 Statistical errors with different SNR values

IOMP-DPD	SNR/dB						
Error	-10	-5	0	5	10	15	20
Target1	0.08%	0.04%	0.00%	0.00%	0.04%	0.00%	0.00%
Target2	0.04%	0.10%	0.83%	0.77%	0.79%	0.47%	0.63%
Target3	0.09%	0.42%	0.02%	0.22%	0.00%	0.00%	0.00%
Target4	0.64%	2.01%	2.51%	1.83%	2.98%	2.80%	2.54%
Target5	2.62%	1.34%	1.23%	1.60%	1.38%	0.48%	0.75%
MUSIC-DPD	SNR/dB						
Error	-10	-5	0	5	10	15	20
Target1	66.80%	30.95%	28.64%	13.51%	2.35%	3.53%	2.75%
Target2	49.53%	24.85%	10.33%	4.41%	4.49%	4.27%	2.89%
Target3	33.32%	18.22%	11.68%	4.67%	2.94%	1.92%	3.61%
Target4	47.55%	27.11%	7.82%	5.95%	4.12%	3.21%	2.01%
Target5	26.65%	13.69%	4.36%	2.30%	2.49%	2.37%	2.12%

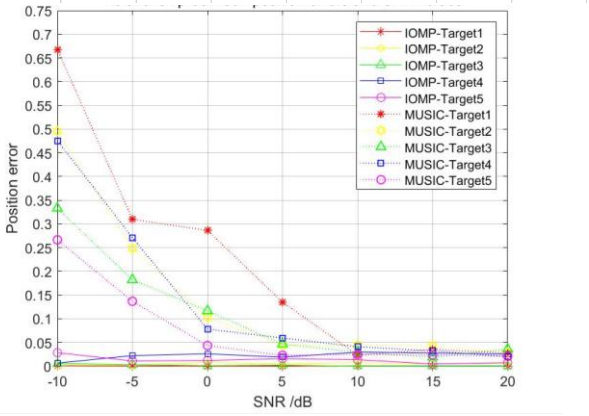

Fig. 6 Corresponding broken line diagram of statistical errors

The statistical positioning errors are shown in Table 4. A broken line diagram of the statistical errors is drawn in Fig. 4 for more intuitive comparison, where the five solid lines represent positioning errors of IOMP-DPD algorithm and the other five dotted lines represent that of MUSIC-DPD algorithm. One color matches one target.

From Table 4, we can observe that all five targets can be located by the improved algorithm with SNR changing from $-10dB$ to $20dB$ while none targets can be located by MUSIC-DPD when $SNR < 0$. That is, the positioning performance of IOMP-DPD is obviously better than that of the other algorithm in low SNR.

Fig. 6 is analyzed from two aspects.

Individually, there is little impact of SNR values on positioning performance of IOMP-DPD algorithm which can be observed by small fluctuation of five solid lines during the whole process of SNR changes while the other algorithm has the opposite conclusion. Almost all five dotted lines start at a large value, drop sharply as SNR increases until it approaches $5dB$, change slowly and tends to stable values gradually.

Overall, it yields smaller positioning errors to locate targets based on IOMP-DPD algorithm than MUSIC-DPD

since almost the five solid lines are all below their corresponding dotted lines except locating $\mathbf{P}_4$ when $SNR = 20dB$, which means it is more susceptible for MUSIC-DPD to SNR values relatively.

That makes sense as high SNR is hardly implemented by observation stations suffering from clutter, noise or other interference factors in actual positioning environment. IOMP-DPD allows for better positioning performance than MUSIC-DPD algorithm in low SNR.

6 Conclusion

We consider two cases of missing information when locating multiple targets and apply CS algorithm to deal with the core problem, as it can reduce the influence of missing information by fusing all observation information instead of processing respectively. We propose an IOMP-DPD algorithm for better positioning performance.

It confirms by simulations that IOMP-DPD substantially reduces the possibility of incomplete location generated by OMP-DPD algorithm and outperforms MUSIC-DPD algorithm in two cases of missing information, illustrated by more targets that can be located and much smaller positioning errors in the same conditions. We have also verified that IOMP-DPD is less sensitive to changes of SNR value and performs much better than MUSIC-DPD algorithm especially in low SNR.

References

H. Gershanoff, Experimental passive range and AOA system shows promise. (angle of arrival passive sensors).

Y.H. Shan, A.N. Wei, Z.K. Sun, F.K. Huang, Passive Location Method Based on Phase Rate of Change, Chinese Journal of Aeronautics, 15 (2002) 49-54.

A. Amar, A.J. Weiss, Direct position determination of multiple radio signals, IEEE International Conference on Acoustics, 2004.

L. Tzafri, A.J. Weiss, High-Resolution Direct Position Determination Using MVDR, IEEE Transactions on Wireless Communications, 15 (2016) 6449-6461.

Weiss, J. A., Direct position determination of narrowband radio transmitters, IEEE, 2 (2004) ii-249-250,ii-251-242.

Z. Huang, J. Wu, Multi-array Data Fusion Based Direct Position Determination Algorithm, 2014 Seventh International Symposium on Computational Intelligence and Design, 2014, pp. 121-124.

J.x. Yin, R.r. Liu, D. Wang, Y. Wu, Direct position determination based on unitary space-time subspace data fusion, 2017 9th International Conference on Wireless Communications and Signal Processing (WCSP), 2017, pp. 1-6.

T. Qin, Z. Lu, B. Ba, D. Wang, A Decoupled Direct Positioning Algorithm for Strictly Noncircular Sources Based on Doppler Shifts and Angle of Arrival, IEEE Access, 6 (2018) 34449-34461.

F. Ma, F. Guo, L. Yang, Direct Position Determination of Moving Sources Based on Delay and Doppler, IEEE Sensors Journal, 20 (2020) 7859-7869.

W. Jiang, W. Xia, S. Zhong, Variable step-size normalized adaptive direct position determination by alternate iteration, 2014 IEEE China Summit & International Conference on Signal and Information Processing (ChinaSIP), 2014, pp. 772-776.

Tingting, Wang, Wei, Ke, Gang, Liu, Sparsity-Based Direct Location Estimation Based on Two-step Dictionary Learning, Communications & Network, (2013).

T. Tirer, A.J. Weiss, Performance Analysis of a High-Resolution Direct Position Determination Method, IEEE Transactions on Signal Processing, 65 (2017) 544-554.

K. Hao, Q. Wan, An Efficiency-improved Tdoa-based Direct Position Determination Method for Multiple Sources, ICASSP 2019 - 2019 IEEE International Conference on Acoustics, Speech and Signal Processing (ICASSP), 2019, pp. 4425-4429.

R.G. Baraniuk, Compressive sensing, Information Sciences and Systems, 2008. CISS 2008. 42nd Annual Conference on, 2008.

S. Subedi, Y.D. Zhang, M.G. Amin, B. Himed, Group sparsity based multi-target tracking in multi-static passive radar systems using Doppler-only measurements, IEEE, (2015).

T. Yumin, W. Zhihui, An adaptive orthogonal matching pursuit algorithm based on redundancy dictionary, 2013 10th International Conference on Fuzzy Systems and Knowledge Discovery (FSKD), 2013, pp. 578-582.

J.A. Luo, W. Zhi, Y.H. Hu, Direct Localization of Multiple Sources in Sensor Array Networks: A Joint Sparse Representation of Array Covariance Matrices Approach, Mobile Ad-Hoc and Sensor Systems (MASS), 2013 IEEE 10th International Conference on, 2013.

X. Lan, K. Barner, Field of experts: Optimal structured Bayesian compressed sensing, 2017 IEEE Global Conference on Signal and Information Processing (GlobalSIP), 2017, pp. 1130-1134.

A. Moro, F. Shang, S. Kidera, T. Kirimoto, Noise robust time of arrival estimation method using hierarchical Bayesian based compressed sensing algorithm, 2016 International Symposium on Antennas and Propagation (ISAP), 2016, pp. 862-863.

H. Ali, S. Ahmed, T.Y. Al-Naffouri, S. Alouini, Reduction of snapshots for MIMO radar detection by block/group orthogonal matching pursuit, 2014 International Radar Conference, 2014, pp. 1-4.

J. Zhao, X. Bai, An improved orthogonal matching pursuit based on randomly enhanced adaptive subspace pursuit, 2017 Asia-Pacific Signal and Information Processing Association Annual Summit and Conference (APSIPA ASC), 2017, pp. 437-441.

S.F. Cotter, B.D. Rao, E. Kjersti, K. Kreutz-Delgado, Sparse solutions to linear inverse problems with multiple measurement vectors, IEEE Transactions on Signal Processing, 53 (2005) 2477-2488.